JTTEE5 15:744-749
DOI: 10.1361/105996306X147054
1059-9630/$19.00 © ASM International

Peer Reviewed

A New Approach to Online Thickness Measurement of Thermal Spray Coatings

A. Nadeau, L. Pouliot, F. Nadeau, J. Blain, S.A. Berube, C. Moreau, and M. Lamontagne

(Submitted March 8, 2006; in revised form June 13, 2006)

In the past 10 years, significant progress has been made in the field of advanced sensors for particle and spray plume characterization. However, there are very few commercially available technologies for the online characterization of the as-deposited coatings. In particular, coating thickness is one of the most important parameters to monitor and control. Current methods such as destructive tests or direct mechanical measurements can cause significant production downtime. This article presents a novel approach that enables online, real-time, and noncontact measurement of individual spray pass thickness during deposition. Micron-level resolution was achieved on various coatings and substrate materials. The precision has been shown to be independent of surface roughness or thermal expansion. Results obtained on typical high-velocity oxyfuel and plasma-sprayed coatings are presented. Finally, current fields of application, technical limitations, and future developments are discussed.

Keywords anamorphic optics, combustion flame spray, high-velocity oxyfuel spray, laser triangulation, layer thickness, plasma spray, thermal spray coatings

1. Introduction

Thermally sprayed coatings are used for many industrial applications in various sectors such as the aerospace, automotive, energy, biomedical, pulp, and paper industries. Their main roles include protection from corrosion, erosion, abrasion, or high temperature (Ref 1-5). Coatings can also be used to promote the biocompatibility of medical implant surfaces, to create functional surfaces, to build new parts, or to repair worn parts (Ref 1, 2, 6-9). For most of these applications, the coating thickness is an important, if not critical, parameter.

On the production floor, precise control of the coating thickness is often a challenge because small deviations in spraying conditions may result in a considerable variation in the deposit efficiency (DE). For example, changes in powder injection profile due to variations in powder morphology or shape, carrier gas pressure, or simple clogging of the injection nozzle will influence the trajectory of the particles in the spray plume, thus influencing particle temperature and velocity, coating structure, and DE (Ref 10-13). Another well-known example is the degradation over time of coating structure and DE in direct current plasma-spraying processes because electrode wear caused by the high torch currents increasingly affects the plasma and therefore the particle properties (Ref 14, 15).

This article was originally published in *Building on 100 Years of Success: Proceedings of the 2006 International Thermal Spray Conference* (Seattle, WA), May 15-18, 2006, B.R. Marple, M.M. Hyland, Y.-Ch. Lau, R.S. Lima, and J. Voyer, Ed., ASM International, Materials Park, OH, 2006.

A. Nadeau, L. Pouliot, F. Nadeau, J. Blain, and **S.A. Berube,** Tecnar, St.-Bruno, QC, Canada; and **C. Moreau** and **M. Lamontagne,** Industrial Materials Institute, Boucherville, QC, Canada. Contact e-mail: anadeau@tecnar.com.

The effect of DE on coating thickness is a major concern of the industry. Significant progress has been achieved over the last 10 years in the development of advanced sensors for online monitoring of critical spray plume parameters such as the velocity, diameter, temperature, and trajectory of the sprayed particles (Ref 10, 16-19). One of the benefits of these sensors is a reduction in DE variations due to tighter control of the spraying conditions.

However, plume-sensing technology has not eliminated the need to verify the final coating thickness, which is still often done by comparing the dimensions of the part before and after coating. The measurements are carried out using mechanical gages such as micrometers or vernier calipers. Other methods such as Eddy current or magnetic induction are also used when the magnetic properties of the coating and/or substrate materials make such measurements possible (Ref 20). These approaches are time consuming as they require the part to be cooled down to room temperature before the measurement is carried out manually by the operator. If the coating thickness is below the target thickness, the part has to be returned to the spray room, reheated, and coated again to reach the desired thickness. On the other hand, if the coating is too thick, the part has to be stripped and recoated.

Several other noncontact thickness gaging methods, such as photothermal and laser-ultrasonic techniques, have been investigated (Ref 20, 21). However, complexity, precision, and implementation costs significantly limit their applicability in actual production environments. Furthermore, ultrasonic techniques require an a priori knowledge of the sound velocity to obtain physical dimensions from echo time intervals. Factors such as porosity and density affect the elastic properties of several types of coatings, such as thermal barrier coatings, and therefore present an additional challenge for ultrasonic methods. Conventional optical triangulation methods have also been investigated. The thickness is obtained by comparing the size of the part before and after coating. This approach is severely limited by other factors affecting the part geometry such as thermal expansion, which is often larger than the coating thickness itself.

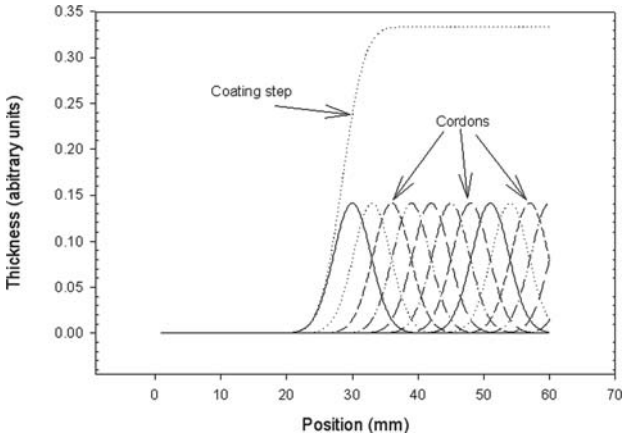

Fig. 1 Formation of the step in the coating profile by the addition of overlapped bell-shaped cordons

As for interferometric techniques, they tend to be difficult to implement in the harsh environment that is intrinsic to thermal spray production floors (Ref 22, 23).

In this article, a novel approach for the online monitoring of the coating thickness in thermal spray processes is presented. Using optical triangulation and differential profilometry, the device measures the coating thickness deposited per pass as it is sprayed. The basic concepts of this new approach are first described, followed by the results obtained offline and online. Current fields of applications and technical limitations are also discussed.

2. Basic Concepts

At the heart of this approach is the idea of measuring the thickness of single spray passes, which can then be added up to obtain the total coating thickness. A single pass produces a smooth step profile over the immediately adjacent, uncoated (or previously coated) surface. The idea is to use simple optical triangulation methods to detect this profile referenced to the adjacent surface, therefore producing a per-pass thickness measurement that is independent of, for example, part motion and thermal expansion. The chosen strategy is to record the profile of the coating at the frontier between the new layer and the previous layer using a laser line projected across the pass edge and captured with a digital charge coupled device (CCD) camera.

Theoretically, on a flat substrate the coating profile along a direction perpendicular to the torch-substrate movement would look like two offset flat lines joined by a smooth, gradual step. This ideal case is illustrated schematically in Fig. 1. The thickness is calculated from the height difference of the two flat lines that represent the previous layer and the new one.

Of course, the profile of a completely coated surface is never perfectly flat. At best, it is mostly flat with some surface roughness, which can vary from 1 to 20 μm and can clearly become a limiting factor for this approach. However, the measurement is done in real time, and the profile is always established on a surface in motion. In other words, this technique implies an intrinsic and crucial surface averaging that diminishes the influence of the roughness while keeping the integrity of the layer step.

The compliant geometries for this concept are relatively flat surfaces in the direction of the profile. Although special algorithms have been developed to compensate for moderately curved surfaces, any curvature higher than the second order within the field of view of the profilometer may limit the precision of the measurement. This effect can be attenuated by the fact that the real step is at a known position in the profile. Initially, applications on flat surfaces such as rollers and cylinders are targeted for the first industrial implementations of this technology.

This method can be used in two different manners. The simplest one uses a sensor in a fixed position, and the profile of the surface is constantly monitored at a specific point in space. As the cordons are sprayed, the layer step will appear and travel through the field of view of the sensor. The thickness can then be measured either by calculating the height of the step or by subtracting two consecutive profiles separated by a short time interval. This last calculation translates into measuring the amount of added matter that was deposited during the time interval. The main advantages of this setup are that the sensor can be mounted far away from the gun trajectory and that the measurement does not depend on a precise a priori knowledge of the substrate shape. It is the simplest way to integrate an online, per pass thickness measurement to control the overall thickness of the coating.

The other configuration offers the advantage of continuous real-time measurement with the sensor attached to the gun. In this case, the technical issues of mounting the sensor close to the gun and on the same displacement unit can become complex. Nevertheless, because this configuration offers possibilities for complete spatial mapping of the final thickness of the coating and real-time monitoring of the DE, most of the work up to now, including online tests, has been steered in that direction.

3. Experimental Setup

To reveal the profile of the layer step, an 80 mm long laser line (660 nm visible wavelength) is projected onto the surface at a fairly low angle (30° above tangent). The image of the laser line on the part surface is recorded with a 10-bit monochrome 1280 × 1024 digital camera that is aimed perpendicular to the observed surface. Anamorphic optics are used to image a rectangular region of 80 mm per 10 mm on the 6.4 mm per 5 mm CCD array.

Like shadows growing longer at sunset, deflection of the laser line by the layer profile is amplified when the projection angle approaches the tangent of the surface. However, the depth of field reduces accordingly. At 30°, the profile is "amplified" by a factor of 2. The depth of field is therefore equal to 5 mm, half of the field of view of the camera in the deflection direction (perpendicular to the laser line). The experimental setup is schematized in Fig. 2. The total weight of the profilometer head is 1.6 kg.

The anamorphic configuration increases the spatial resolution along the deflection direction. Due to the high anamorphic ratio, optical aberrations are present in the other direction (perpendicular to the line), but they do not affect the analysis of the layer step. Furthermore, special algorithms are applied to the raw image to compensate for the geometric deformations caused by large-aperture optics with short focal lengths.

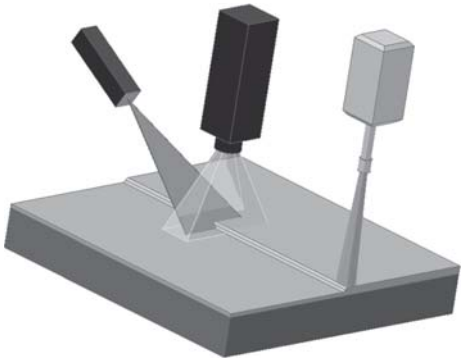

Fig. 2 The laser line is aimed at the new layer frontier, and its deflection is imaged by a digital camera. The height of the deflection, which corresponds to the layer thickness, is obtained through image analysis.

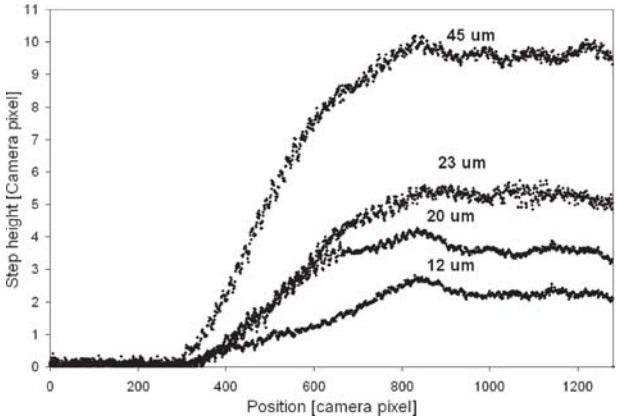

Fig. 3 Raw profiles of four different step heights from 12 to 45 μm. Those results were recorded on a previously coated moving surface.

4. Results and Discussion

The sensor was tested in different environments, and the results are reported below on measurements carried out both offline and online. Online tests were carried out in a laboratory and in an industrial production plant to further validate the technology.

4.1 Offline Laboratory Tests

The very first validation tests of the concept were made offline using precoated flat samples with precalibrated steps. Those experiments confirmed that the measurement of a 5 μm step was possible with the surface-averaging effect of a moving sample. They also helped in establishing optimal operating parameters such as the line projection angle, anamorphic ratio of the camera lens, and its digital resolution.

Figure 3 shows raw profiles of four different high-velocity oxyfuel (HVOF) coating steps varying from 12 to 45 μm. The smooth profile was recorded on a surface moving at a typical spray-gun speed. As mentioned earlier, the intrinsic surface averaging of this technique greatly diminishes the profile ripple caused by surface roughness.

The first task of the image analysis algorithm is to find the position of the line within the CCD array. This position calculation must have a micron level precision to be able to measure a single pass of a few microns with a reasonable accuracy. For example, with the 1024 pixel lines of the CCD capturing a 10 mm field of view and using a 30° angle for the line projector, a 10 μm layer step will induce a deflection of about 2 pixels. Therefore, the required precision corresponds to a subpixel resolution of the line position.

The offline development was then shifted to axis symmetric geometries like cylinders. Aluminum cylinders 4 in. in diameter were produced and coated with WC-12%Co by HVOF and yttria-stabilized zirconia by plasma spray. Each sample was divided into four sections coated with an increasing number of layers to obtain three well-defined steps per cylinder. The steps were mechanically measured with a micrometer, and some samples were cut and measured with a scanning electron microscope. The results of those measurements are presented in Table 1.

Table 1 Height of the three coating steps between the four sections of the four cylinders used in the offline tests

Cylinder	Step No. 1, μm	Step No. 2, μm	Step No. 3, μm
HVOF No. 1	45 ± 3	20 ± 3	9 ± 3
HVOF No. 2	23 ± 3	12 ± 3	4.5 ± 3
Plasma No. 1	50 ± 3	25 ± 3	12 ± 3
Plasma No. 2	25 ± 3	12 ± 3	6 ± 3

A continuous measurement of the step was recorded to verify the stability of the reading. The results are displayed in Fig. 4. The results show, on average, a very good stability. However, individual profiles sometimes were observed to differ significantly from the step model presented in Fig. 1. These isolated cases represented <5% of the profiles. A numerical averaging of 10 to 20 profiles was sufficient to diminish the effect of bad profiles and to reach a precision of a few microns. The current sampling rate of 10 profiles per second translated into a reaction time between 1 and 2 s. The algorithm was also adjusted to reject profiles with unusual steps. The rejection criterion was based on the position of the step in the screen as well as on its height. The minimum and maximum height limits were dynamically set in accordance with the standard deviation and the average value of the last 50 profiles.

The results obtained offline on the precoated cylinders demonstrated the achievement of the targeted resolution with the measurement of a 5 μm single-pass step of WC-Co coating with a signal-to-noise ratio above 10. This ratio is calculated by dividing the difference of amplitude between the 5 μm level and the noise level by the standard deviation of the noise. Figure 5 presents the linear relation between the optical measurement and the physically measured step height.

Once calibrated from the HVOF data points of Fig. 5, the system was tested with the plasma-sprayed cylinders. The thickness measured by the sensor was in very good agreement with the real values of the steps, and therefore confirmed that the measurement is independent of the coating material and process.

4.2 Online Laboratory Tests

With the offline tests, key issues like minimum resolution, calibration, and material-independent measurements were con-

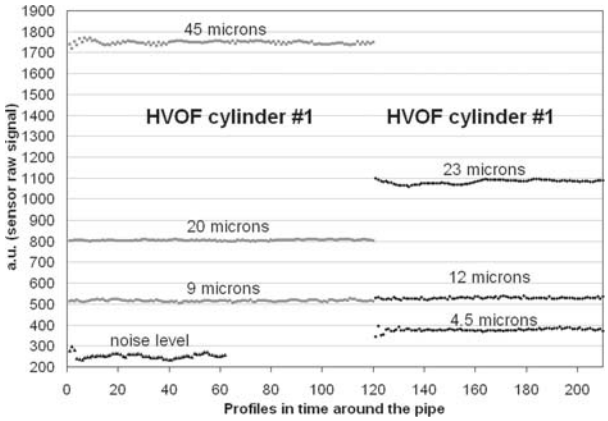

Fig. 4 Continuous recording of coating step profiles on two rotating, WC-12%Co precoated, 4 in. diameter aluminum cylinders. The step heights vary from 5 to 45 μm.

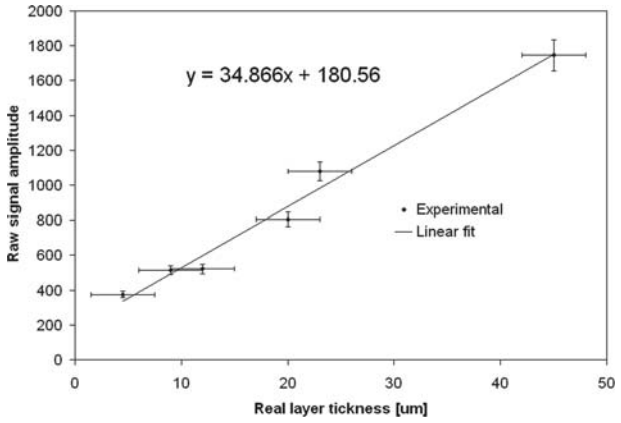

Fig. 5 The profilometer raw amplitude as a function of the coating step thickness. The linear fit is used for the calibration of the system.

firmed. Online tests were essential to develop the real-time configuration of the sensor. Mechanical vibrations, hot gas birefringence, and thermal expansion are some of the factors that could affect the sensor in a production environment. A total of five cylinders were sprayed with multiple layers of WC-12%Co. Spray parameters like the gun speed, the cylinder rotation velocity, and the powder feed rate were adjusted to deposit various layers with thicknesses ranging from 8 to 40 μm. The sensor was mounted with the gun directly on the robot using a special bracket that is able to handle both. To protect the sensor from the spray plume, additional metallic shielding and air blowing was added to the online installation.

A first series of online results was obtained on a 7 in. diameter, 20 in. long steel cylinder coated with a total of nine layers. Each layer was monitored by the sensor. The same spraying parameters were applied to the first six layers, and the approximated thickness deposited per pass was about 13 μm. For the last three layers, the powder feed rate was doubled.

Figure 6 shows the real-time thickness measurement of all nine passes. It also shows the noise level recorded with a live gun without powder feed. The online noise levels were observed to be significantly higher. Most of this increase is attributed to the

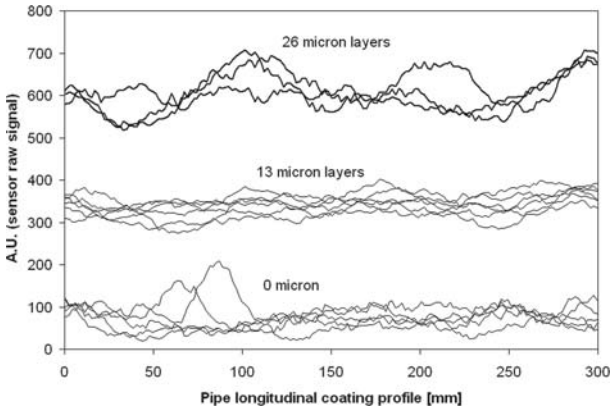

Fig. 6 Real-time online measurements of the layer thickness during deposition. The six lower curves indicate the measurement output with a zero powder feed rate. The six middle curves indicate the measurement of approximately 13 μm layers. The three upper curves are the measurements with the powder feed rate doubled.

fluctuations in the profile due to the refraction effects created by the random circulation of hot gasses in the sensor field of view. Similar variations could be induced offline simply by blowing hot air in front of the device. However, noise levels were low enough not to compromise the correlation between the measured thickness signal and the powder feed rate. In fact, the sensitivity of the sensor is still excellent and comparable to the offline sensitivity. The source of the observed fluctuations of the measurement is still not fully understood. Of course, its effect can be further reduced by increasing averaging.

The general tendency of the 200 thickness measurements per pass shown in Fig. 6 is linear and stable. An averaging of 200 profiles may be a good starting point for further online experiments. This, of course, will increase the reaction time of the sensor to approximately 20 s, which is still more than sufficient for the intended purpose. The final coating thickness is given by adding every layer.

Figure 7 shows the profile of the total coating thickness given by the sensor and by a destructive scanning electron microscopy measurement. On the same figure are the separate totals of the first six thin passes and the last three thick passes.

The second online measurements were performed on four aluminum cylinders measuring 6 in. in diameter and 20 in. in length. Each one of them received six layers of HVOF-sprayed WC-12%Co. The main goal was to compare the relationship between the thickness and the measurement with online results. To do so, the spraying conditions were modified from one sample to the other to get four different total coating thicknesses. Destructive measurements were performed on the cylinders at various locations to determine their actual thickness profiles.

The results, shown in Fig. 8, confirm the linear relationship between the sensor measurements and the coating thickness. However, some measurements presented variations that were not correlated with the actual thickness profile. With further analysis, a few surface regions were found where the coating profile strongly differed from the ideal step function. Those exceptions seem to be related to the spraying conditions and are more significant with smaller cylinder diameters. They could also be attributed to the surface condition of the cylinders as well.

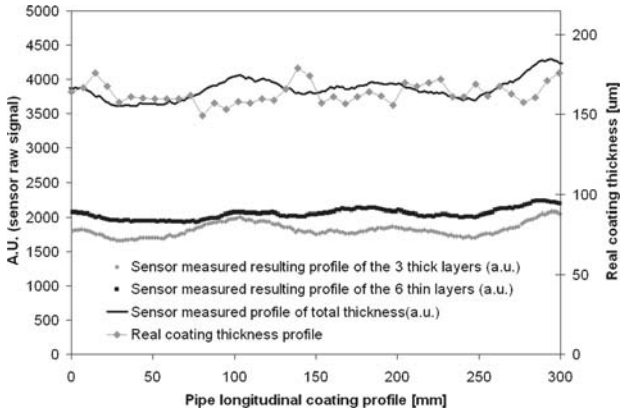

Fig. 7 In the lower part of the graph, the thick black line is the sum of all three thick layers, and the thick gray line is the sum of all six thin layers. The calculated sum of these two lines is plotted as the continuous thin black line at the top of the graph. It exhibits a variance that is comparable to the destructive measurements of the final coating, displayed as gray diamonds.

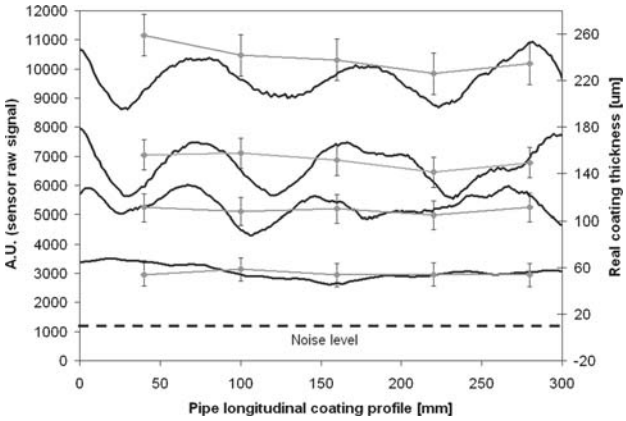

Fig. 8 The black lines show the four different coating profiles measured by the sensor. The black dotted line shows the noise level of the sensor, which offsets the linear calibration equation. The gray data points plot the real thickness profiles of the coating (measured by optical microscopy) for each sample. The error bars represent the standard deviation of the local thickness around each measurement point.

Figure 8 also shows that the oscillations are important and are synchronized in the two thicker samples. The cylinder rotation speed and the gun speed were the same in the two conditions. Only the powder feed rate was increased. Fortunately, for usual spraying speeds used in HVOF spraying, those variations are much less apparent. Once again, the results are in favor of the longer averaging approach for real-time monitoring. Nevertheless, experiments are underway to understand the causes of those variations and to establish a more robust algorithm for the detection/rejection of bad profiles that could bias the thickness measurement.

4.3 Online Industrial Tests

A precommercial version of the sensor (LayerGauge; Tecnar Automation Ltd., St.-Bruno, QC, Canada) was used to perform online measurements in an industrial environment (Hazelett Strip-Casting Corporation). The Hazelett belt technology for liquid metal casting requires thermal spray coatings to protect the belt from the high thermal load involved in such a process. Following the interest of the company in online monitoring of the coating thickness, numerous measurements were carried out to validate the compatibility of the sensor with their application. Figure 9 shows the sensor performing a live measurement as the coating edge reaches the center of the sensor field of operation.

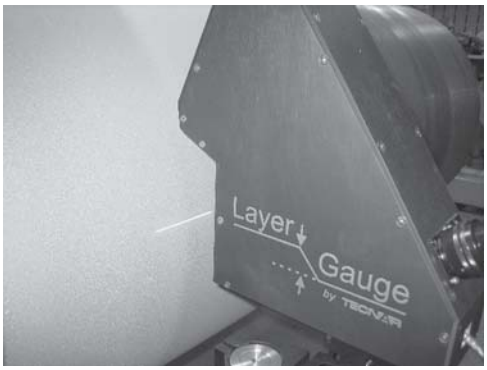

Fig. 9 Online measurement of the bond coat thickness as it is deposited on an industrial strip casting metallic belt

Two thermal spray processes have been monitored, namely, plasma and combustion flame spraying. Online measurements were performed with a stationary sensor while the coating edge was passing in front of its field of view. Because the longitudinal displacement velocity of the spray gun was relatively slow (2 cm/min), several discrete measurements were acquired within the time frame of a single spray pass. A total of four measurements was carried out over the width of the belt for the plasma spray coating (bond coat), and five for the flame spray coating (top coat).

The results, summarized in Fig. 10, are in excellent agreement with the offline measurements, although the latter have limited precision compared with the optical sensor measurements. The offline measurements were made by means of an Eddy current probe for the top coat and with a precision micrometer for the bond coat. Work is currently under way to fully correlate the distribution of the optical sensor results with the actual thickness of the coating.

5. Conclusions

A novel approach based on optical triangulation to achieve the noncontact online thickness measurement of thermal spray coatings was presented. The sensor monitors the layer thickness as it is deposited. The required micron level resolution was easier to achieve for offline measurements on precoated cylinders than for live online tests, where it was limited to approximately 5 μm. The online experimental and industrial tests have confirmed the functionality of the sensor in a production environment. The measurement was found to be independent of the coating/substrate nature, the surface roughness, or the thermal expansion of the coated part. Further beta-test site implementations are under way to explore the possible fields of application of that technology.

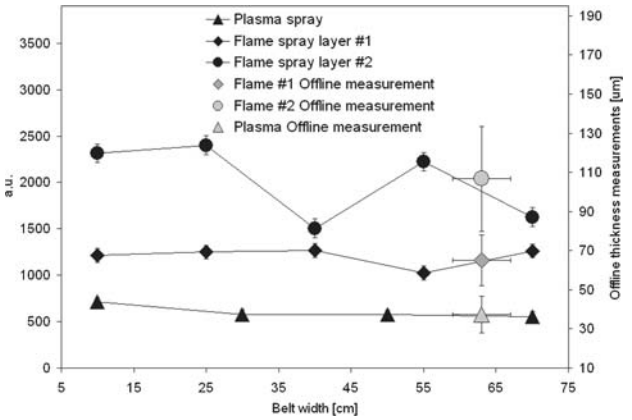

Fig. 10 Online measurements performed at an industrial thermal spray site. The dots represent discrete measurements along a metallic belt. Three layers were monitored, one plasma-sprayed and two combustion flame-sprayed.

Acknowledgments

The authors would like to acknowledge the financial support from the IRAP Canadian program. They would also like to acknowledge the outstanding support received from Frédéric Belval, Sylvain Bélanger, Michel Thibodeau, and Jean-François Alarie, without whom that work would not have been possible. Finally, the authors would like to express their sincere appreciation to Hazelett personnel for giving them the opportunity to test that new technology in their facility.

References

1. J.R. Davis, Ed., *Handbook of Thermal Spray Technology,* ASM international, 2004
2. L. Pawlowski, *The Science and Engineering of Thermal Spray Coatings,* John Wiley, New York 1995
3. R.A. Miller, *Thermal Barrier Coatings for Aircraft Engines: History and Direction,* NASA Report CP-3312, W. J. Brindley, Ed., National Aeronautics and Space Administration, Glenn Research Center, Cleveland, OH, 1995, p 17-34
4. McCune, R.C., Thermal Spraying of Cylinder Bore Surfaces for Aluminum Engine Blocks, *Weld. J.,* 1995, August, p 41-47
5. Z. Dongming, J.A. Nesbitt, C.A. Barrett, T.R. McCue, and R.A. Miller, Furnace Cyclic Oxidation Behavior of Multicomponent Low Conductivity Thermal Barrier Coatings, *J. Thermal Spray Technol.,* 2004, **13**(1), p 84-92
6. R.S. Lima, K.A. Khor, H. Li, P. Cheang, and B.R. Marple, HVOF Spraying of Nanostructured Hydroxyapatite for Biomedical Applications, *Mater. Sci. Eng. A,* 2005, **396**(1-2), p 181-187
7. Y. Fuxing and O. Akira, The Photocatalytic Activity and Photo-Absorption of Plasma Sprayed TiO_2–Fe_3O_4 Binary Oxide Coatings, *Surf. Coat. Technol.,* 2002, **160,** p 62-67
8. M. Krauss, D. Bergmann, U. Fritsching, and K. Bauckhage, In-Situ Particle Temperature, Velocity and Size Measurements in the Spray Forming Process, *Mater. Sci. Eng. A,* 2002, **A326**(1), p 154-164
9. J. Richard, Gambino, M.M. Raja, S. Sampath, and R. Greenlaw, Plasma-Sprayed Thick-Film Anisotropic Magnetoresistive (AMR), *IEEE Sens. J.,* 2004, **4**(6), p 764-767
10. P. Fauchais, A. Vardelle, and B. Dussoobs, Quo Vadis Thermal Spraying, *J. Thermal Spray Technol.,* 2001, **10**(1), p 105-110
11. M. Prystay, P. Gougeon, and C. Moreau, Structure of Plasma-Sprayed Zirconia Coatings Tailored by Controlling the Temperature and Velocity of the Sprayed Particles, *J. Thermal Spray Technol.,* 2001, **10**(1), p 67-75
12. B. Champagne and S. Dallaire, Particle Injection in Plasma Spraying, *Thermal Spray: Advances in Coatings Technology,* D.L. Houck, Ed., Sept 14-17, 1987 (Orlando, FL), ASM International, 1988, p 25
13. A. Vardelle, P. Fauchais, K.-I. Li, B. Dussoubs, and N.J. Thermelis, Controlling Particle Injection in Plasma Spraying, *J. Thermal Spray Technol.,* 2001, **10**(2), p 267-284
14. L. Leblanc and C. Moreau, The Long-Term Stability of Plasma Spraying, *J. Thermal Spray Technol.,* 2002, **11**(3), p 380-386
15. C. Moreau and L. Leblanc, Characterization and Process Control for High Performance Thermal Spray Coatings, *Key Eng. Mater.,* 2001, **197,** p 27-57
16. J.F. Bisson, C. Moreau, L. Pouliot, J. Blain, and F. Nadeau, Ensemble In-Flight Particle Diagnostics Under Various Spraying Conditions, *Thermal Spray 2001: New Surfaces for a New Millennium,* C.C. Berndt, Ed., May 28-30, 2001 (Singapore), ASM International, 2001, p 705-714
17. C. Moreau, P. Gougeon, M. Lamontagne, V. Lacasse, G. Vaudreuil, and P. Cielo, *Thermal Spray Industrial Applications,* C.C. Berndt and S. Sampath, Ed., June 20-24, 1994 (Boston, MA), ASM International, 1994, p 431
18. W.D. Swank, J.R. Fincke, and D.C. Haggard, *Advances in Thermal Spray Science & Technology,* C.C. Berndt and S. Sampath, Ed., Sept 11-15, 1995 (Houston, TX), ASM International, 1995, p 111
19. J. Vaffulainen, E. Hamalainen, R. Hernberg, P. Vuoristo, and T. Mantyla, Novel Method for In-Flight Particle Temperature and Velocity Measurements in Plasma Spraying Using a Single CCD Camera, *J. Thermal Spray Technol.,* 2001, **10**(1), p 94-104
20. L. Fabbri and M. Oksanen, Characterization of Plasma-Sprayed Coatings Using Nondestructive Evaluation Techniques: Round-Robin Test Results, *J. Thermal Spray Technol.,* 1999, **8**(2), p 263-272
21. M. Viens, D. Drolet, A. Blouin, J.-P. Monchalin, and C. Moreau, *Thermal Spray: Practical Solutions for Engineering Problems,* C.C. Berndt, Ed., Oct 7-11, 1996 (Cincinnati, OH), ASM International, 1996, p 947
22. C. Moreau, Towards a Better Control of Thermal Spray Processes, *Thermal Spray: Meeting the Challenges of the 21st Century,* C. Coddet, Ed., May 25-29, 1998 (Nice, France), ASM International, 1998, p 1681-1693
23. P. Cielo, *Optical Techniques for Industrial Inspection,* Academic Press, Inc., San Diego, CA, 1988, p 195